Available online at www.sciencedirect.com

ScienceDirect

journal homepage: www.jfda-online.com

Original Article

7-N-Acetylcysteine-pyrrole conjugate—A potent DNA reactive metabolite of pyrrolizidine alkaloids

Xiaobo He, Liang Ma, Qingsu Xia, Peter P. Fu *

National Center for Toxicological Research, U.S. Food and Drug Administration, Jefferson, Arkansas, United States

ARTICLE INFO

Article history:
Received 29 July 2016
Available online 10 September 2016

Keywords:
DHP
LC-ES-MS/MS
7-*N*-acetylcysteine-DHP
pyrrolizidine alkaloid

ABSTRACT

Plants containing pyrrolizidine alkaloids (PAs) are widespread throughout the world and are the most common poisonous plants affecting livestock, wildlife, and humans. PAs require metabolic activation to form reactive dehydropyrrolizidine alkaloids (dehydro-PAs) that are capable of alkylating cellular DNA and proteins, form (±)-6,7-dihydro-7-hydroxy-1-hydroxymethyl-5*H*-pyrrolizine (DHP)-DNA and DHP-protein adducts, and lead to cytotoxicity, genotoxicity, and tumorigenicity. In this study, we determined that the metabolism of riddelliine and monocrotaline by human and rat liver microsomes in the presence of *N*-acetylcysteine both produced 7-*N*-acetylcysteine-DHP (7-NAC-DHP) and DHP. Reactions of 7-NAC-DHP with 2′-deoxyguanosine (dG), 2′-deoxyadenosine (dA), and calf thymus DNA in aqueous solution followed by enzymatic hydrolysis yielded DHP-dG and/or DHP-dA adducts. These results indicate that 7-NAC-DHP is a reactive metabolite that can lead to DNA adduct formation.

1. Introduction

To date, more than 660 pyrrolizidine alkaloids (PAs) and PA *N*-oxides have been identified in over 6000 plant species distributed worldwide. About half of these phytochemicals contain a C2–C3 double bond at the necine base and are hepatotoxic; many of them are genotoxic and tumorigenic in experimental animals [1–7]. It has long been established that PA-containing plants are probably the most common poisonous plants affecting livestock, wildlife, and humans [1,6].

PAs are biologically inactive and require metabolism to exert toxicity. Upon metabolism, PAs generate dehydropyrrolizidine alkaloids (dehydro-PAs) as the primary reactive pyrrolic metabolites [3,6]. Dehydro-PAs are highly unstable, they can be readily hydrolyzed into (±)-6,7-dihydro-7-hydroxy-1-hydroxymethyl-5*H*-pyrrolizine (DHP), and alkylate cellular DNA and proteins to produce DHP-DNA and DHP-protein adducts, leading to cytotoxicity, genotoxicity, and tumorigenicity (Fig. 1) [1,6].

We recently determined that PA-induced liver tumors in rats were mediated by a set of four DHP-DNA adducts, i.e., a pair of epimers of 7-hydroxy-9-(deoxyguanosin-N^2-yl)dehydrosupinidine adducts (designated as DHP-dG-3 and DHP-dG-4), and a pair of epimers of 7-hydroxy-9-(deoxyadenosin-N^6-yl)dehydrosupinidine adducts (designated as DHP-dA-3 and

* *Corresponding author*. National Center for Toxicological Research, U.S. Food and Drug Administration, Jefferson, Arkansas 72079, United States.
E-mail address: peter.fu@fda.hhs.gov (P.P. Fu).
http://dx.doi.org/10.1016/j.jfda.2016.08.001

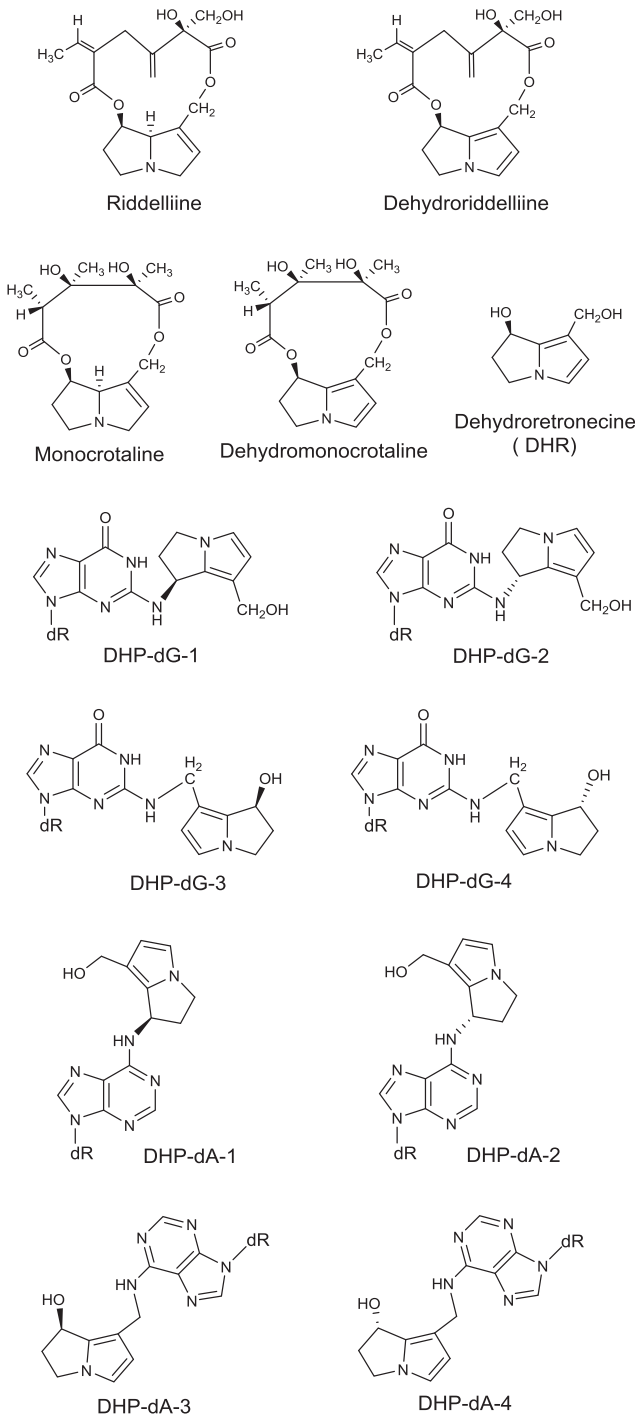

Figure 1 – Structures of PAs, dehydro-PAs, DHP, DHP-dG-1, DHP-dG-2, DHP-dG-3, DHP-dG-4, DHP-dA-1, DHP-dA-2, DHP-dA-3, and DHP-dA-4 adducts. dA = 2′-deoxyadenosine, dG = 2′-deoxyguanosine, DHP = (±)-6,7-dihydro-7-hydroxy-1-hydroxymethyl-5*H*-pyrrolizine, PA = pyrrolizidine alkaloids.

DHP-dA-4) (Fig. 1) [8]. Based on this and previous findings in our laboratory [2,9–18], we proposed that DHP-dG-3, DHP-dG-4, DHP-dA-3, and DHP-dA-4 adducts are biomarkers of PA exposure and potential biomarkers of PA-induced carcinogenicity [8]. In addition, a pair of epimers of 7-(deoxyguanosin-N^2-yl)dehydrosupinidine adducts (designated as DHP-dG-1 and DHP-dG-2 adducts) and a pair of epimers of 7-(deoxyadenosin-N^6-yl)dehydrosupinidine adducts (designated as DHP-dA-1 and DHP-dA-2 adducts) were also produced *in vitro* (Fig. 1) [8,10,19].

Dehydro-PAs have a very short half-life in aqueous systems, only around 0.31–5.36 seconds [20], and thus may not be the principal reactive metabolites to bind to cellular DNA leading to genotoxicity and carcinogenicity. Consequently, there may be other reactive metabolites that can also bind to cellular DNA to initiate cytotoxicity, genotoxicity, and carcinogenicity [6].

7-Glutathionyl-(±)-6,7-dihydro-1-hydroxymethyl-5*H*-pyrrolizine (7-GS-DHP) is a metabolite formed *in vivo* and *in vitro* [21–25]. We recently found that 7-GS-DHP can bind with calf thymus DNA to form the eight above described DHP–DNA adducts, e.g., DHP-dG-1, DHP-dG-2, DHP-dG-3, DHP-dG-4, DHP-dA-1, DHP-dA-2, DHP-dA-3, and DHP-dA-4 adducts [26]. We have also found that 7-cysteine-DHP is a new metabolite formed from the metabolism of riddelliine and monocrotaline by human and rat liver microsomes and can bind with calf thymus DNA to form the same set of DHP-dG and DHP-dA adducts [27]. These results suggest that both 7-GS-DHP and 7-cysteine-DHP are reactive metabolites that can lead to DNA adduct formation.

Estep et al [28] reported that 7-*N*-acetylcysteine-DHP (7-NAC-DHP) was detected in the urine of male Sprague-Dawley rats administered ^{14}C-monocrotaline or ^{14}C-senecionine. They suggested that 7-NAC-DHP was formed in the liver and excreted in the urine [28]. In the present study, we determined that metabolism of monocrotaline and riddelliine by human and rat liver microsomes in the presence of *N*-acetylcysteine generated 7-NAC-DHP. We subsequently determined that reaction of 7-NAC-DHP with 2′-deoxyguanosine (dG), 2′-deoxyadenosine (dA), and calf thymus DNA generated DHP-dG and/or DHP-dA adducts. These results suggest that, similar to 7-GS-DHP and 7-cysteine-DHP, 7-NAC-DHP adduct can be a potential DNA reactive metabolite of PAs and may potentially initiate liver tumors in rodents and humans.

2. Materials and methods

2.1. Chemicals

N-acetylcysteine, calf thymus DNA (sodium salt, Type I), nuclease P1, micrococcal nuclease, spleen phosphodiesterase, NADPH, 2′-deoxyguanosine (dG), and 2′-deoxyadenosine (dA) were purchased from Sigma-Aldrich (St. Louis, MO, USA). Dimethylformamide, acetonitrile, potassium carbonate, chloroform, diethyl ether, and phosphate buffered saline were obtained from Fisher Scientific (Pittsburg, PA, USA). AX 1-X8 anion exchange resin was purchased from Bio-Rad (Hercules, CA, USA). All solvents used were high performance liquid chromatography (HPLC) grade.

Dehydromonocrotaline was synthesized by dehydrogenation of monocrotaline in chloroform with *o*-chloranil, as previously described [19]. DHP was obtained from the metabolism

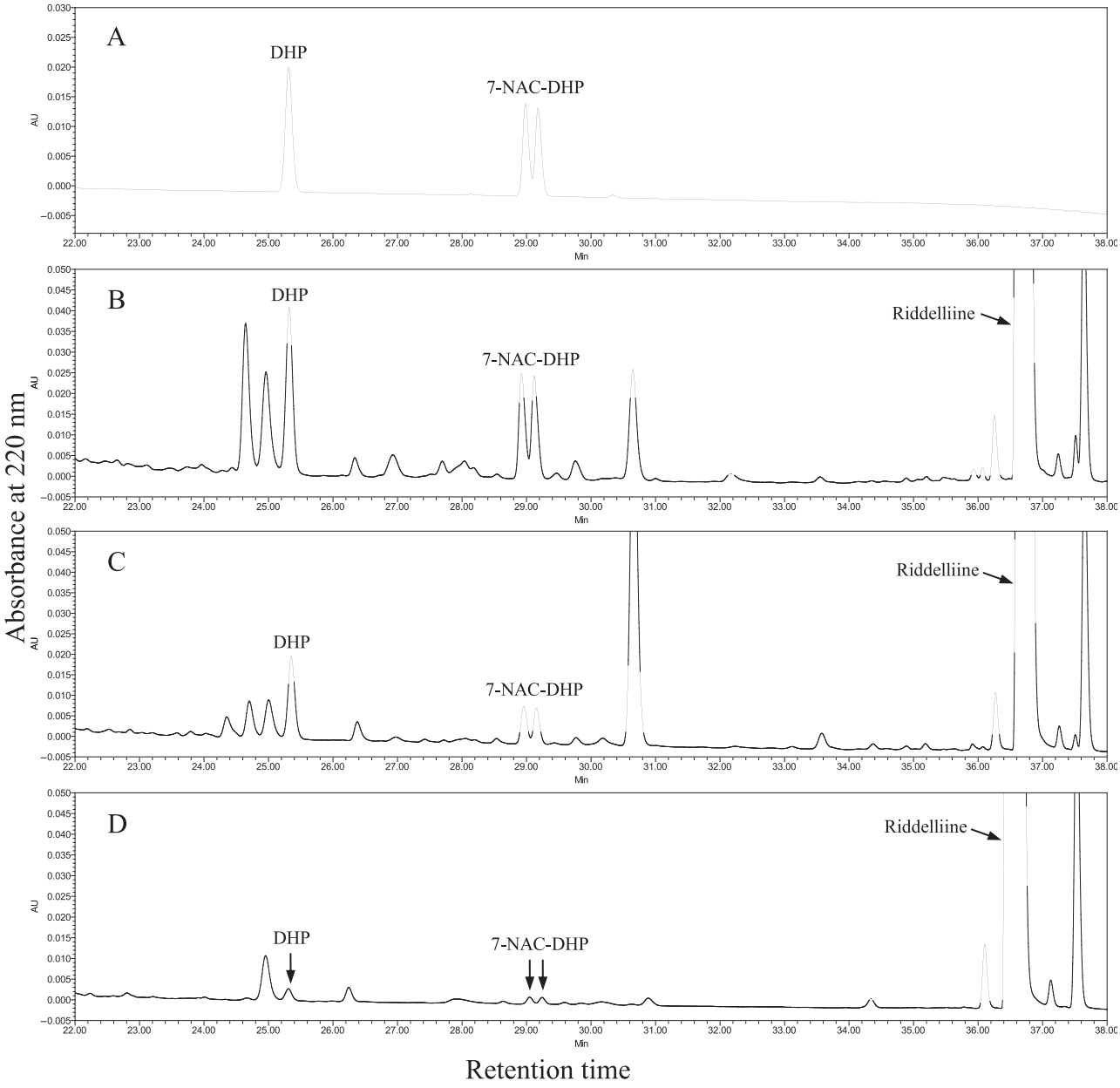

Figure 2 – HPLC profiles of 7-NAC-DHP and DHP obtained from (A) organic synthesis; and from metabolism of riddelliine in the presence of *N*-acetylcysteine by (B) male human liver microsomes; (C) male rat liver microsomes; and (D) male rat liver microsomes without the addition of NADPH. DHP = (±)-6,7-dihydro-7-hydroxy-1-hydroxymethyl-5H-pyrrolizine, HPLC = high performance liquid chromatography, NAC = *N*-acetylcysteine.

of riddelliine by rat liver microsomes [27]. DHP-dG-1, DHP-dG-2, DHP-dG-3, DHP-dG-4, DHP-dA-1, DHP-dA-2, DHP-dA-3, and DHP-dA-4 adducts were synthesized as previously described [10,19]. Isotopically labeled DHP-[$^{15}N_5$]dG and DHP-[$^{15}N_5$, $^{13}C_{10}$]dA adducts, used as internal standards for quantitation of DHP-dG and DHP-dA adducts by liquid chromatography-tandem mass spectrometry (LC/MS/MS), were synthesized as described previously [8,10].

Male human liver microsomes and male Fischer 344 rat liver microsomes were purchased from Bioreclamation IVT (Baltimore, MD, USA). DNA concentrations were determined spectrophotometrically.

2.2. *Synthesis of 7-NAC-DHP adduct*

N-acetylcysteine (125 mg, 0.77 mmol) dissolved in 5 mL acetone was added dropwise to a solution of dehydromonocrotaline (200 mg, 0.62 mmol) in 20 mL acetone at ambient temperature. The reaction mixture was stirred at ambient temperature for 2 hours, and then poured into 100 mL phosphate buffered saline (0.1 M, pH = 7.4). After the solvent was removed under reduced pressure, the resulting residue was dissolved in 3 mL 0.005% formic acid and ammonia solution (pH 8), and loaded to a C18 open column (20 g), first eluting with 50 mL 0.005% formic acid and ammonia solution (pH 8) to remove the salts and *N*-

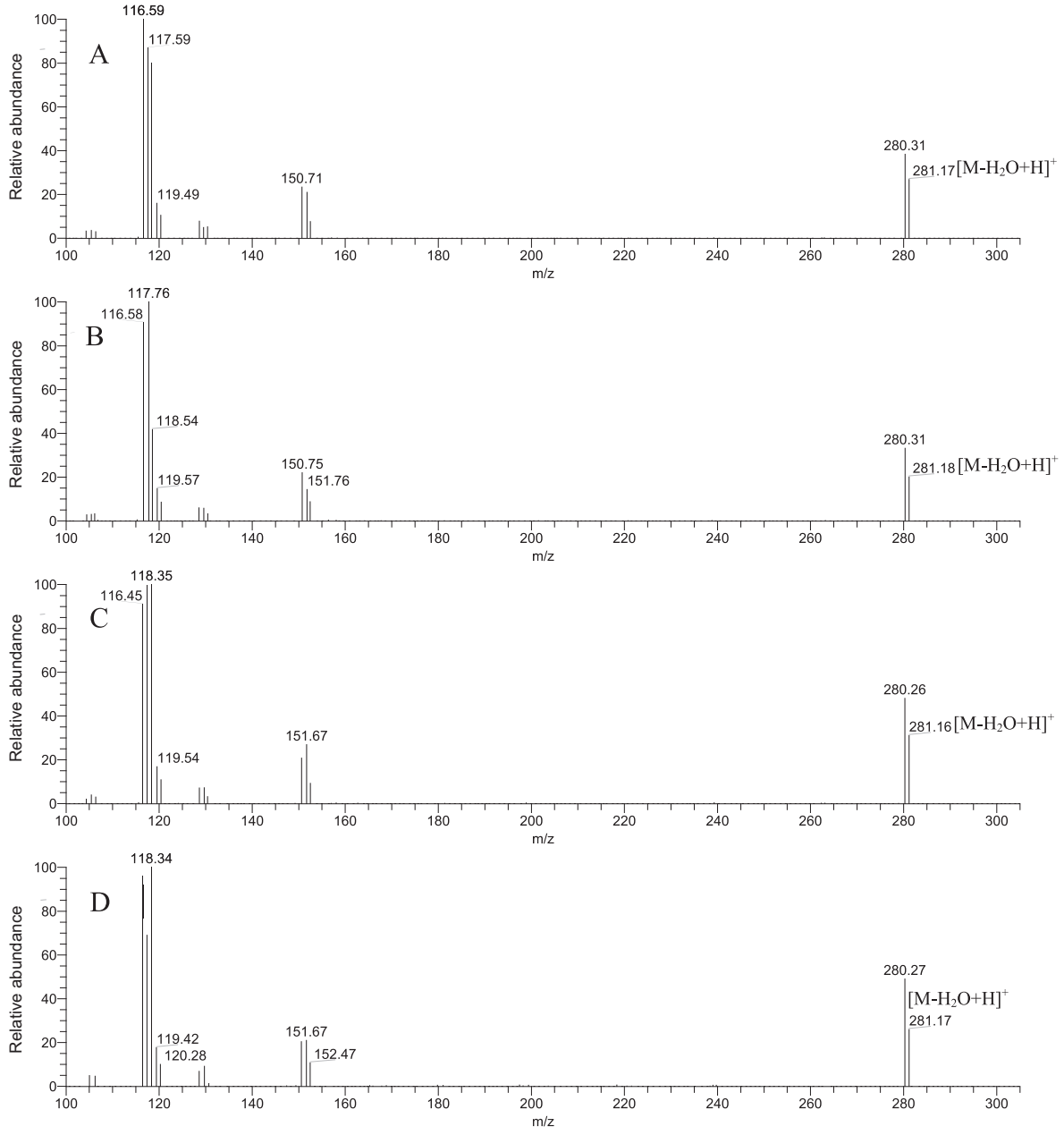

Figure 3 – Electrospray positive ion/product ion mass spectra of 7-NAC-DHP from (A) organic synthesis; and in the chromatographic peak eluting at 28.85–29.25 minutes in Fig. 2 obtained from the results of the metabolism of riddelliine in the presence of *N*-acetylcysteine by (B) male human liver microsomes; (C) male rat liver microsomes; and (D) male rat liver microsomes without the addition of NADPH. The product ions of the $[M - H_2O + H]^+$ m/z 281 were acquired with a collision energy of 10 eV. DHP = (±)-6,7-dihydro-7-hydroxy-1-hydroxymethyl-5*H*-pyrrolizine, NAC = *N*-acetylcysteine.

acetylcysteine, then with 100 mL 4% acetonitrile in 0.005% formic acid and ammonia solution (pH 8) to collect the products. The 7-NAC-DHP adduct-containing fractions were concentrated and purified by HPLC with the following conditions: column (Phenomenex Luna (Phenomenex Inc., Torrance, CA, USA) C18 (2), 250 mm × 10 mm), flow rate (3 mL/min), mobile phase (5% acetonitrile in 0.005% formic acid and ammonia solution (pH 8), isocratic), monitored at 220 nm. This resulted in a pure product identified as a pair of epimeric 7-NAC-DHP in a nearly equal ratio. The product ion scan mass spectrum had an $[M - H_2O + H]^+$ ion at m/z 281 and characteristic fragment ions at m/z 116–119 and m/z 150–152. The structure was confirmed by ^1H nuclear magnetic resonance (NMR) spectral data. The ^1H NMR spectral assignments of 7-NAC-DHP adduct are as follows:

7-NAC-DHP. ^1H NMR (500 MHz, D_2O): δ 2.50 (m, 1H, H6a), 2.98-2.88 (m, 1H, H6b), 3.05 (m, 1H, H2′), 3.15 (m, 1H, H2′), 3.62 (m, 1H, H1′), 3.88 (m, 1H, H1′), 3.92 (m, 1H, H5b), 4.02 (m, 1H, H5a), 4.52–4.44 (m, 3H, H7, H9), 6.17 (d, J = 2.6 Hz, 1H, H2), 6.62 (d, J = 2.6 Hz, 1H, H3).

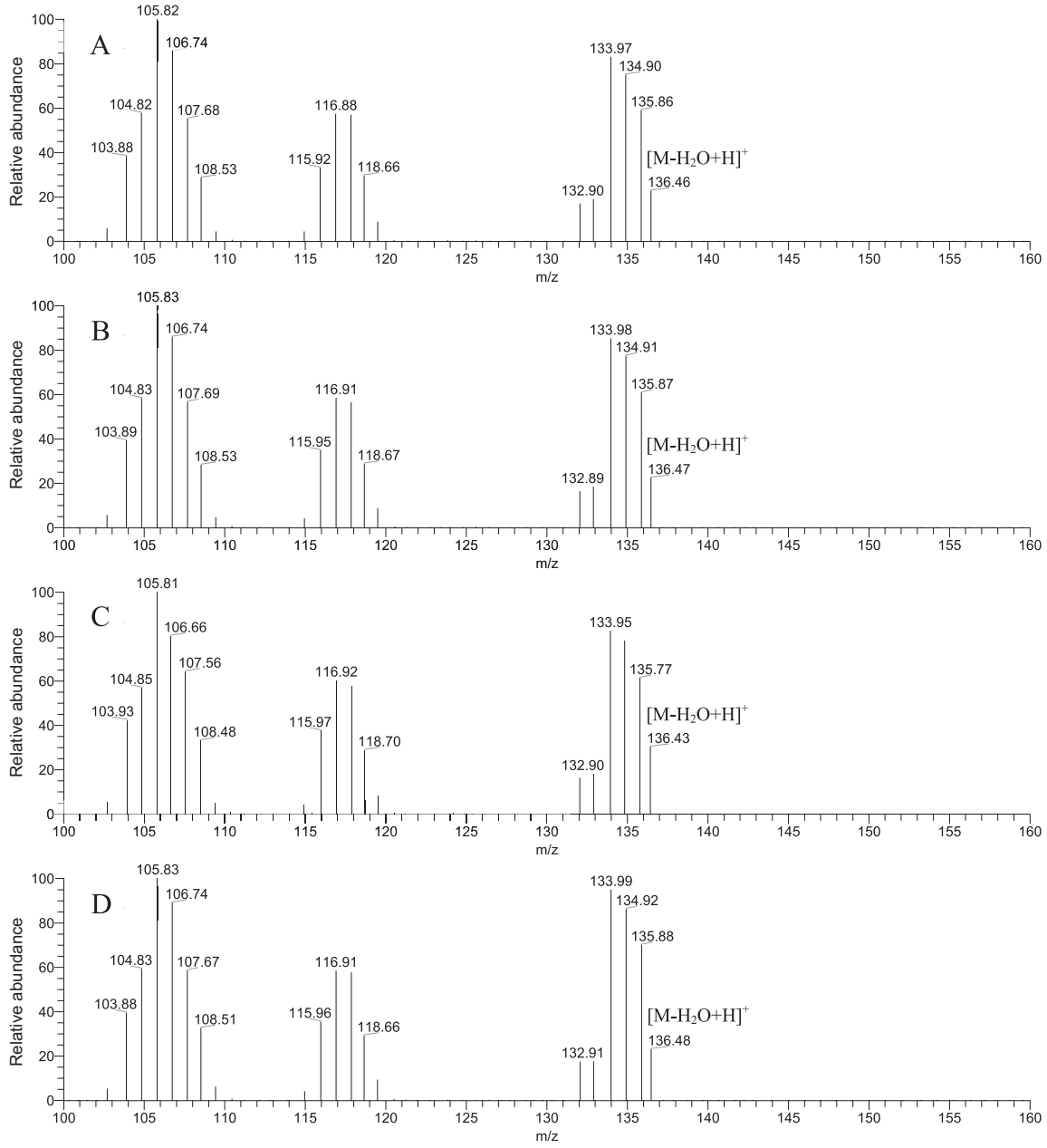

Figure 4 – Electrospray positive ion/product ion mass spectra of DHP from (A) organic synthesis; and in the chromatographic peak eluting at 25.3 minutes in Fig. 2 obtained from the metabolism of riddelliine in the presence of *N*-acetylcysteine by (B) male human liver microsomes; (C) male rat liver microsomes; and (D) male rat liver microsomes in the absence of NADPH, The product ions of the $[M - H_2O + H]^+$ m/z 136 were acquired with a collision energy of 22 eV. DHP = (±)-6,7-dihydro-7-hydroxy-1-hydroxymethyl-5*H*-pyrrolizine.

2.3. *Formation of 7-NAC-DHP from metabolism of riddelliine and monocrotaline by human and rat liver microsomes in the presence of N-acetylcysteine*

The metabolism of riddelliine (or monocrotaline) by male F344 rat microsomes in the presence of *N*-acetylcysteine was conducted in a 1 mL incubation volume containing 100 mM sodium phosphate buffer (pH 7.6), 5 mM magnesium chloride, 1 mM NADPH, 500 μM riddelliine (or monocrotaline), 2 mM *N*-acetylcysteine, and 1 mg of rat liver microsomal protein at 37°C for 60 minutes. After the incubation, the mixture was centrifuged at 105,000 g for 30 minutes at 4°C to remove microsomal proteins. The supernatant was collected, and aliquots of 50 μL were directly subjected to HPLC-UV analysis. The metabolism of riddelliine and monocrotaline by male human liver microsomes was conducted similarly.

The metabolism of riddelliine (or monocrotaline) by male F344 rat microsomes in the presence of *N*-acetylcysteine, but without the addition of NADPH, was also performed.

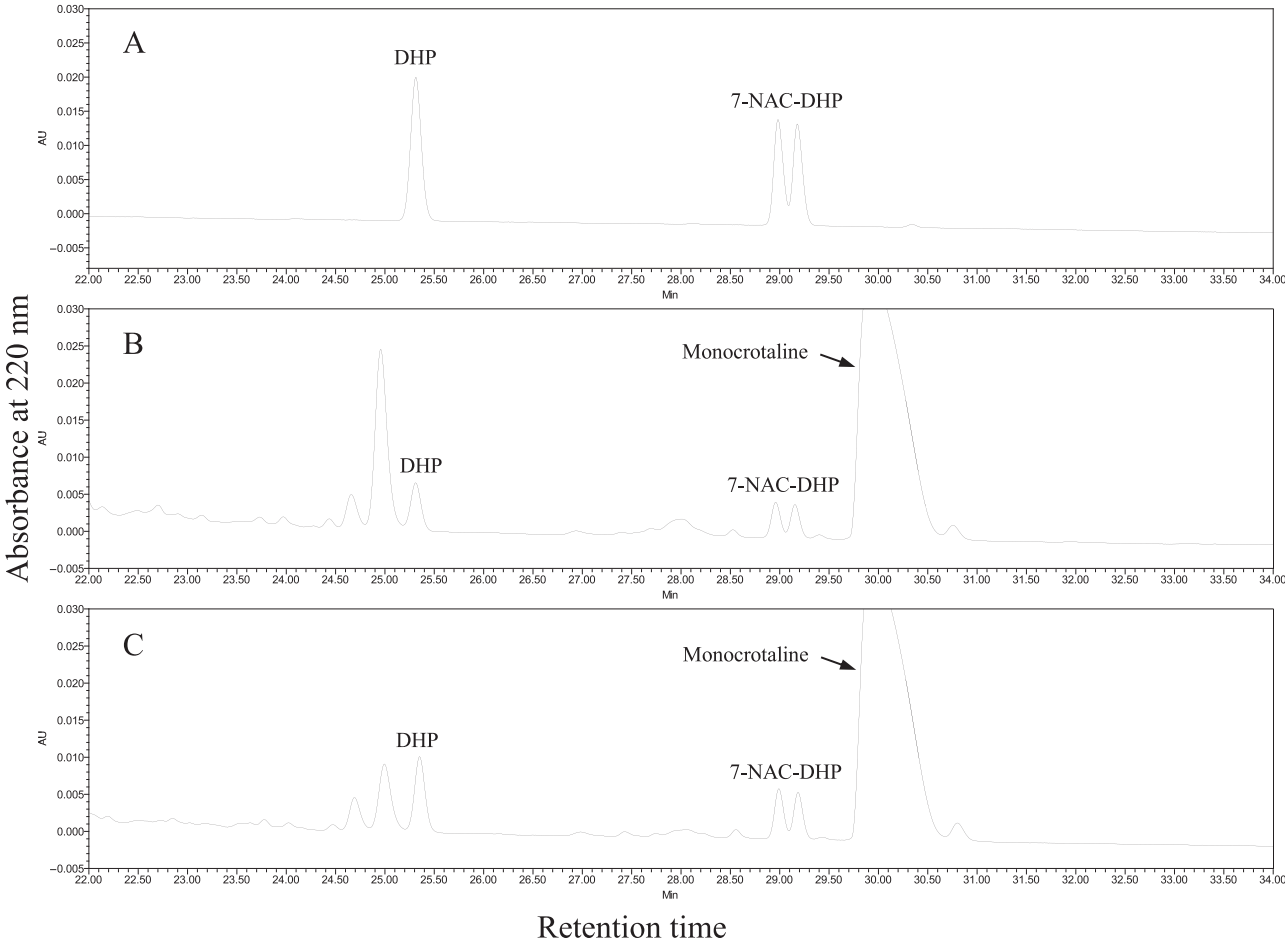

Figure 5 – HPLC profiles of 7-NAC-DHP and DHP from (A) organic synthesis; and from metabolism of monocrotaline in the presence of N-acetylcysteine by (B) male human liver microsomes; and (C) male rat liver microsomes. DHP = (±)-6,7-dihydro-7-hydroxy-1-hydroxymethyl-5H-pyrrolizine, NAC = N-acetylcysteine.

2.4. *Reaction of 7-N-acetylcyteine-DHP with dG and dA*

Following the experimental conditions previously reported for the reaction of 7-GS-DHP with dG [26], 1 mL of reaction mixture containing 1 mM 7-NAC-DHP and 2 mM dG in 0.01% formic acid and ammonia solution (pH 8) was kept at 37°C with shaking. The reaction products were monitored by HPLC for 1, 3, and 5 days, respectively, with the following conditions: Phenomenex Luna C18 (2) column, 250 mm × 4.6 mm, isocratic elution with 12% acetonitrile in water at a flow rate of 1 mL/min, monitored at 256 nm for DHP-dG and 220 nm for DHP, respectively.

The reaction of 7-NAC-DHP with dA was similarly conducted with the exceptions: monitored at 269 nm for DHP-dA, and isocratic elution with 15% acetonitrile in water.

2.5. *Reaction of 7-NAC-DHP with calf thymus DNA*

A 1 mL of reaction mixture containing 500 μM 7-NAC-DHP and 1 mg calf thymus DNA in 0.01% formic acid and ammonia solution (pH 8) was kept at 37°C with shaking for 1, 3, and 5 days. After the reaction, 100 μL aliquots of the reaction mixtures (containing 100 μg DNA) were enzymatically hydrolyzed to nucleotides with micrococcal nuclease, spleen phosphodiesterase, and nuclease P1 as previously described [26] before LC/MS/MS analysis. Reactions were conducted in triplicate.

2.6. *HPLC- electrospray-MS/MS analysis of metabolites and reaction products*

Liquid chromatography. A Finnigan Surveyor HPLC system (ThermoFinnigan, San Jose, CA, USA) was coupled with the TSQ mass spectrometer. The samples were loaded onto a Luna 3 μm C18 column (4.6 × 150 mm, Phenomenex) with a gradient of acetonitrile and water (containing 2 mM ammonium acetate, pH 7.0) and a flow rate of 300 μL/min. The gradient began with 3% acetonitrile for 10 minutes followed by a linear gradient up to 20% acetonitrile over the next 25 minutes. The samples were maintained at 5°C in the autosampler during the entire analysis.

Mass spectrometry. A TSQ Quantum Ultra Triple Stage Quadrupole MS/MS System (ThermoFinnigan, San Jose, CA, USA) was equipped with an atmospheric pressure ionization electrospray (ES) interface. The instrument was operated in positive ion mode. The spray voltage was set to 3000 V, vaporizer temperature to 300°C, and capillary temperature to 300°C.

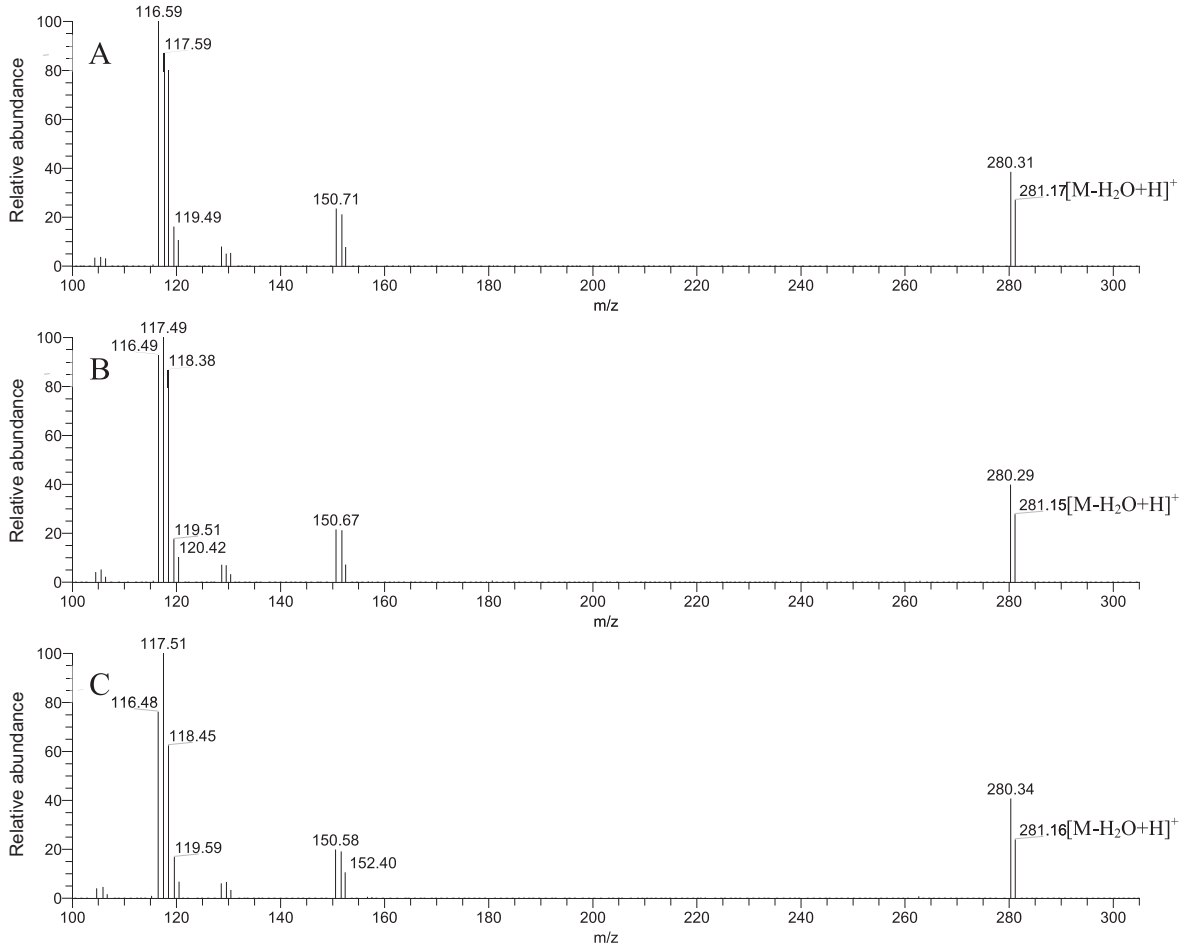

Figure 6 – Electrospray positive ion/product ion mass spectra of 7-NAC-DHP from (A) organic synthesis; and in the chromatographic peak eluting at 28.85–29.25 minutes in Fig. 5 obtained from the metabolism of monocrotaline in the presence of *N*-acetylcysteine by (B) male human liver microsomes; and (C) male rat liver microsomes. The product ions of the $[M - H_2O + H]^+$ m/z 281 were acquired with a collision energy of 10 eV. DHP = (±)-6,7-dihydro-7-hydroxy-1-hydroxymethyl-5*H*-pyrrolizine, NAC = *N*-acetylcysteine.

Nitrogen was used as the sheath gas and the auxiliary gas; argon was the collision gas. Nitrogen pressures of the sheath and auxiliary gases were set to 30 and 5 (arbitrary units), respectively.

2.7. *Quantitation of DHP-dG and DHP-dA adducts by LC/MS/MS analysis*

Liquid chromatography. A Finnigan Surveyor HPLC system was coupled with the TSQ mass spectrometer. The samples were loaded onto a reverse phase column (ACE 3 C18, 4.6 mm × 150 mm, 3 μm; MAC–MOD Analytical, Chadds Ford, PA, USA) with a gradient of methanol and water (containing 2 mM ammonium acetate; pH 5) with a flow rate of 0.3 mL/min. The gradient began with 15% methanol for 5 minutes, followed by a linear gradient up to 65% methanol over the next 35 minutes. The samples were maintained at 5°C in the autosampler during the entire analysis.

Mass spectrometry. The same TSQ Quantum Ultra Triple Stage Quadrupole ES-MS/MS System (ThermoFinnigan) was used to perform for the DHP-DNA adduct analysis. The spray voltage was 3000 V, vaporizer temperature was 400°C, and capillary temperature was 280°C. Nitrogen pressure of sheath and auxiliary gas was 30 and 5 (arbitrary units), respectively. The argon collision gas pressure was 1.5 m Torr, the collision energy was 17 eV for DHP-dG and its internal standard; and 21 eV for DHP-dA and its internal standard. The selected reaction monitoring (SRM) scheme was employed involving transitions of the $[M+H]^+$ precursor ions to selected product ions, with the following values: m/z 403 → 269 for DHP-dG adducts; m/z 408 → 274 for DHP-[$^{15}N_5$]dG internal standards; m/z 387 → 253 for DHP-dA adducts; m/z 402 → 263 for DHP-[$^{15}N_5$, $^{13}C_{10}$]dA internal standards.

3. Results

3.1. *Metabolism of riddelliine by human and rat liver microsomes in the presence of N-acetylcysteine*

The metabolism of riddelliine by male human liver microsomes in the presence of *N*-acetylcysteine was conducted and the metabolites were separated by reversed-phase HPLC

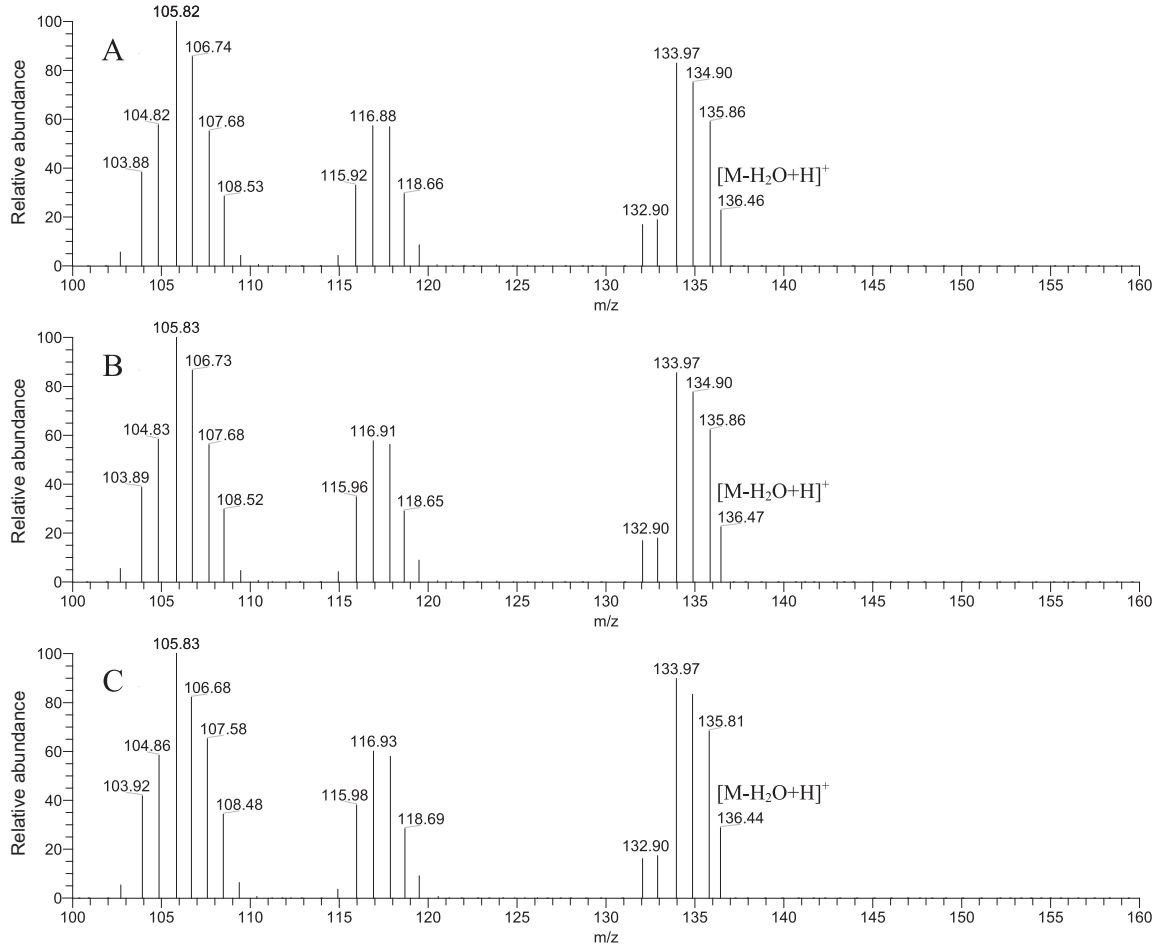

Figure 7 – Electrospray positive ion/product ion mass spectra of DHP from (A) organic synthesis; and in the chromatographic peak eluting at 25.3 minutes in Fig. 5 obtained from the metabolism of monocrotaline in the presence of *N*-acetylcysteine by (B) male human liver microsomes; and (C) male rat liver microsomes. The product ions of the $[M - H_2O + H]^+$ m/z 136 were acquired with a collision energy of 22 eV. DHP = (±)-6,7-dihydro-7-hydroxy-1-hydroxymethyl-5*H*-pyrrolizine.

(Fig. 2). The material in the two chromatographic peaks eluting at 28.85–29.25 minutes (Fig. 2B) had HPLC retention times, UV-visible-absorption spectra (data not shown), and mass product ion scan profiles (Fig. 3B) identical to those of the synthesized 7-NAC-DHP standard (Figs. 2A and 3A). The mass product ion scan spectra of the 7-NAC-DHP synthetic standard (Fig. 3A) and this metabolite (Fig. 3B) both had an $[M - H_2O + H]^+$ ion at m/z 281 and characteristic fragment ions at m/z 117–119, and m/z 151–152. Based on these spectral results, the material eluting at 28.85–29.25 minutes in Fig. 2B was unequivocally identified as 7-NAC-DHP. The chromatographic peak eluting at 36.6 minutes in Fig. 2B was the recovered riddelliine substrate.

The chromatographic peak eluting at 25.3 minutes (Fig. 2B) had a HPLC retention time, UV-visible-absorption spectrum (data not shown), and mass product ion scan profile (Fig. 4B) identical to those of the DHP standard (Figs. 2A and 4A). The ES positive product ion mass spectra had an $[M - H_2O + H]^+$ ion at m/z 136 and the characteristic fragment ions at m/z 104–119 (Figs. 4A–D). Thus, the material eluting at 25.3 minutes in Fig. 2B was unequivocally identified as DHP.

The metabolism of riddelliine by male F344 rat liver microsomes in the presence of *N*-acetylcysteine was conducted similarly. The HPLC profile is shown in Fig. 2C. Similar to the description above for the metabolism of riddelliine by male human liver microsomes, comparison of their HPLC retention times, UV-visible absorption spectra (data not shown), and mass spectra of the resulting metabolites with those of the synthetic standards, the metabolites eluting at 25.3 minutes and 28.85–29.25 minutes (Fig. 2C) were identified as DHP and 7-NAC-DHP, respectively.

The metabolism of riddelliine by male F344 rat liver microsomes in the presence of *N*-acetylcysteine and in the absence of NADPH was conducted in parallel. As the metabolism result shown in Fig. 2D and compared with metabolism in the presence of NADPH (Fig. 2C), the yields of both 7-NAC-DHP and DHP decreased drastically in the absence of exogenous NADPH, consistent with the requirement of NADPH as a cofactor for cytochrome P450 enzyme activity. These results indicate that the metabolic formation of 7-NAC-DHP was by the reaction of dehydroriddelliine with *N*-acetylcysteine and that the formation of DHP is mainly by the hydrolysis of dehydroriddelliine.

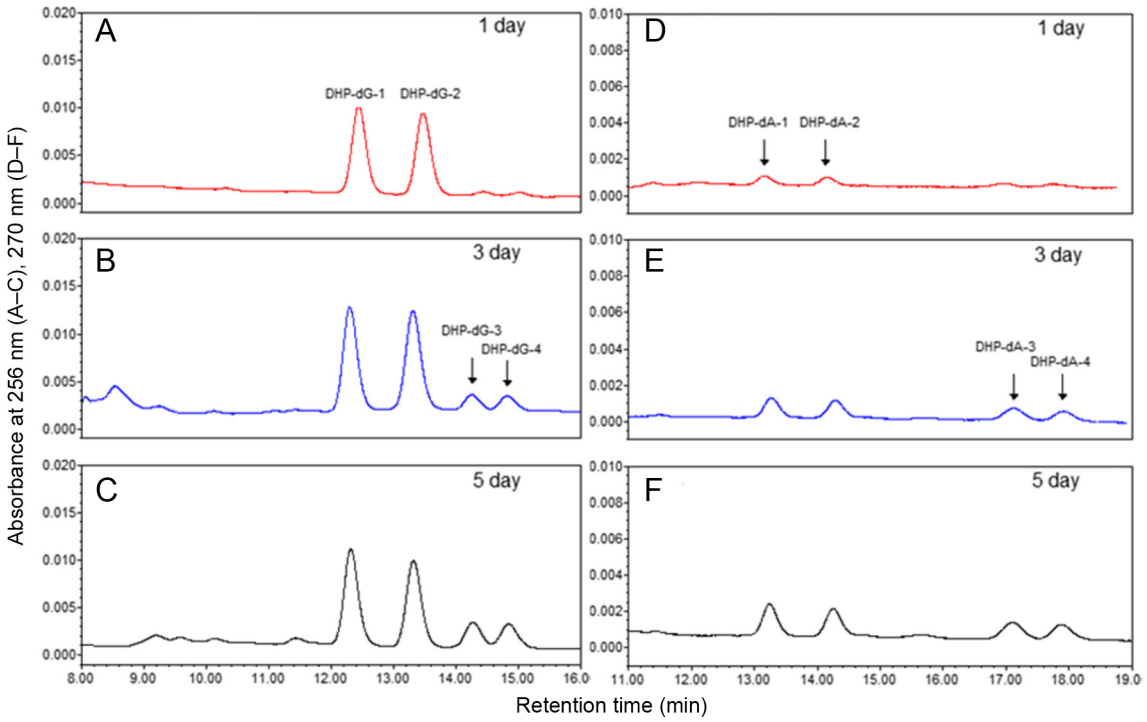

Figure 8 – HPLC profiles of reactions of 7-NAC-DHP with dG and dA for 1, 3, and 5 days: (A–C) detection of DHP-dG adducts monitored at 256 nm; and (D–F) detection of DHP-dA adducts monitored at 269 nm. For reaction conditions, see Materials and methods section. dA = 2′-deoxyadenosine, dG = 2′-deoxyguanosine, DHP = (±)-6,7-dihydro-7-hydroxy-1-hydroxymethyl-5*H*-pyrrolizine.

3.2. *Metabolism of monocrotaline by human and rat liver microsomes*

The metabolism of monocrotaline by male human and rat liver microsomes in the presence of *N*-acetylcysteine was conducted. Similar to the metabolism of riddelliine, the metabolites were separated by HPLC (Figs. 5B and 5C) and identified by comparison of their HPLC retention times (Figs. 5B and 5C), UV-visible absorption spectra (data not shown), and mass spectrometric profiles (Figs. 6 and 7) with those of the synthetic standards. Both 7-NAC-DHP and DHP were similarly identified.

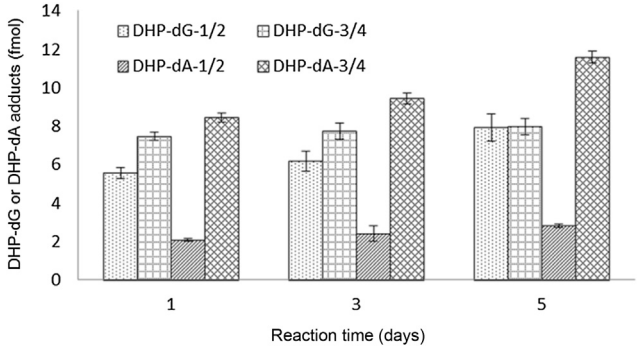

Figure 9 – The formation of DHP-dG and DHP-dA adducts from reaction of 7-NAC-DHP with calf thymus DNA for 1, 3, and 5 days. dA = 2′-deoxyadenosine, dG = 2′-deoxyguanosine, DHP = (±)-6,7-dihydro-7-hydroxy-1-hydroxymethyl-5*H*-pyrrolizine, NAC = *N*-acetylcysteine.

3.3. *DHP-dG and DHP-dA adducts formed from reaction of 7-NAC-DHP and dG and dA*

The reaction of 7-NAC-DHP with dG was conducted for 1, 3, and 5 days. At Day 1, DHP-dG-1 and DHP-dG-2 were formed while DHP-dG-3 and DHP-dG-4 were not detected. At Day 3, DHP-dG-3 and DHP-dG-4 were generated. At Day 5, DHP-dG-1 and DHP-dG-2 were formed as the predominant adducts (Figs. 8A–C). The reaction yields of DHP-dG-1 and DHP-dG-2 adducts increased in a time dependent manner. The identity of the DHP-dG products was confirmed by LC-MS/MS analysis and compared with synthetic standards.

The formation of DHP was monitored at 220 nm by HPLC and confirmed with the HPLC retention time and mass of the authentic DHP. The yield of DHP was also increased in a time dependent manner (data not shown).

Reaction of 7-NAC-DHP and dA was similarly conducted. As shown in Fig. 8D–F, the formation of DHP-dA-1 and DHP-dA-2 was faster than DHP-dA-3 and DHP-dA-4. On the basis of the previous assumption that the molar extinction coefficients of DHP-dA-1, DHP-dA-2, DHP-dA-3, and DHP-dA-4 are identical [19], the yields of DHP-dA-1 and DHP-dA-2 are higher than DHP-dA-3 and DHP-dA-4. Similar to the reaction of 7-NAC-DHP with dG, DHP was also produced (data not shown).

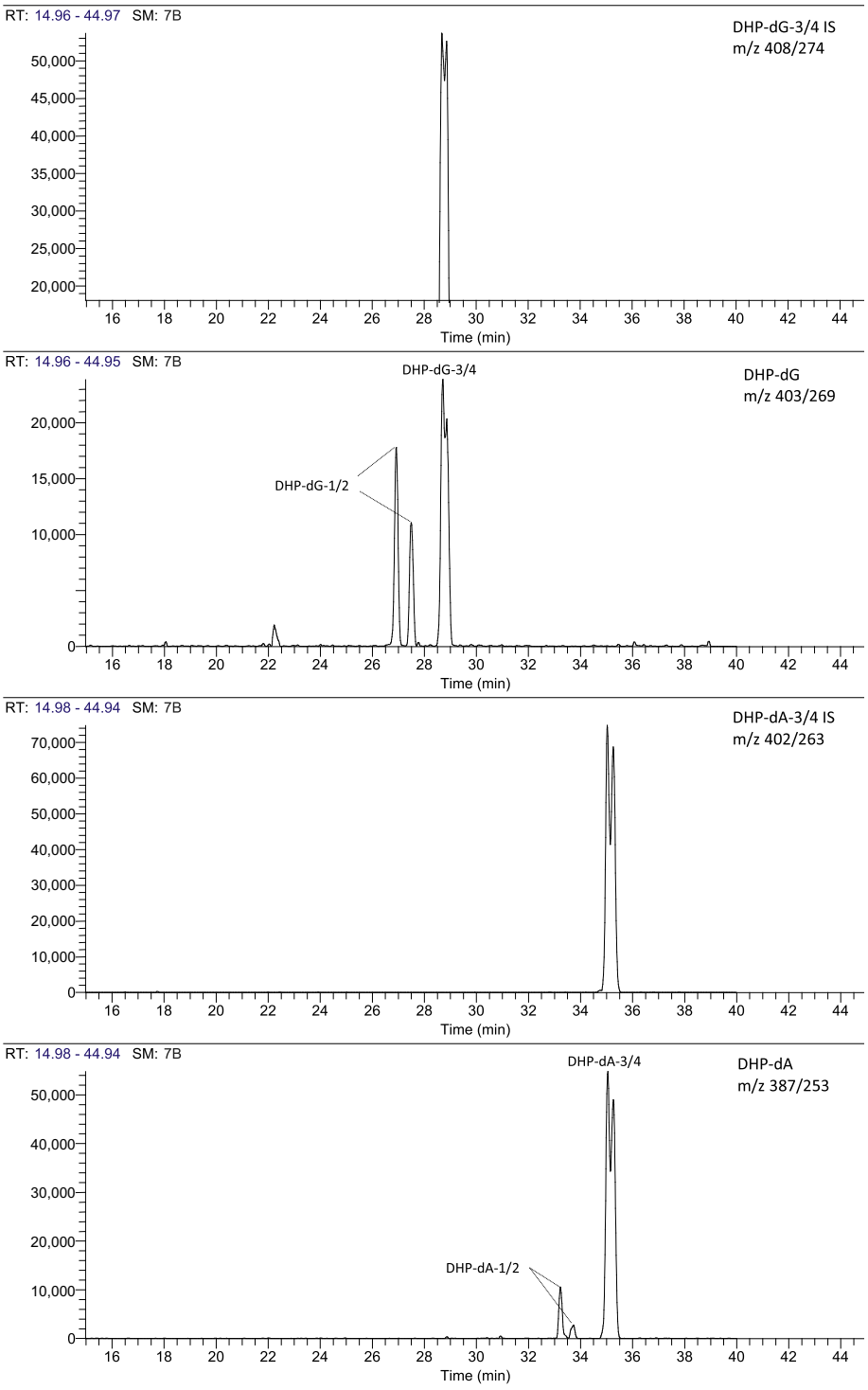

Figure 10 – LC/MS SRM chromatograms of DHP-dG and DHP-dA adducts formed from the reaction of 7-NAC-DHP with calf thymus DNA for 3 days. dA = 2′-deoxyadenosine, dG = 2′-deoxyguanosine, DHP = (±)-6,7-dihydro-7-hydroxy-1-hydroxymethyl-5*H*-pyrrolizine, IS = DHP-[$^{15}N_5$]dG and DHP-[$^{15}N_5$, $^{13}C_{10}$]dA labeled internal standards, LC/MS = liquid chromatography/mass spectrometry, NAC = N-acetylcysteine, SRM = selected reaction monitoring.

3.4. *LC-ES-MS/MS analysis of DHP-dG and DHP-dA adducts formed from reaction of 7-NAC-DHP and calf thymus DNA*

The DHP-dG and DHP-dA adducts formed from reaction of 7-NAC-DHP with calf thymus DNA in ammonium hydroxide solution at pH 8 for 1, 3, and 5 days were quantitated by LC-ES-MS/MS analysis using SRM mode with the use of DHP-[$^{15}N_5$]dG-3/4 and [$^{15}N_5$, $^{13}C_{10}$]dA-3/4 as internal standards. At Day 1, all the DHP-dG and DHP-dA adducts were formed (Fig. 9). At Day 5, DHP-dA-1/2 was formed in the lowest yield. DHP-dA-3/4 adducts were the predominant adducts and their formation was

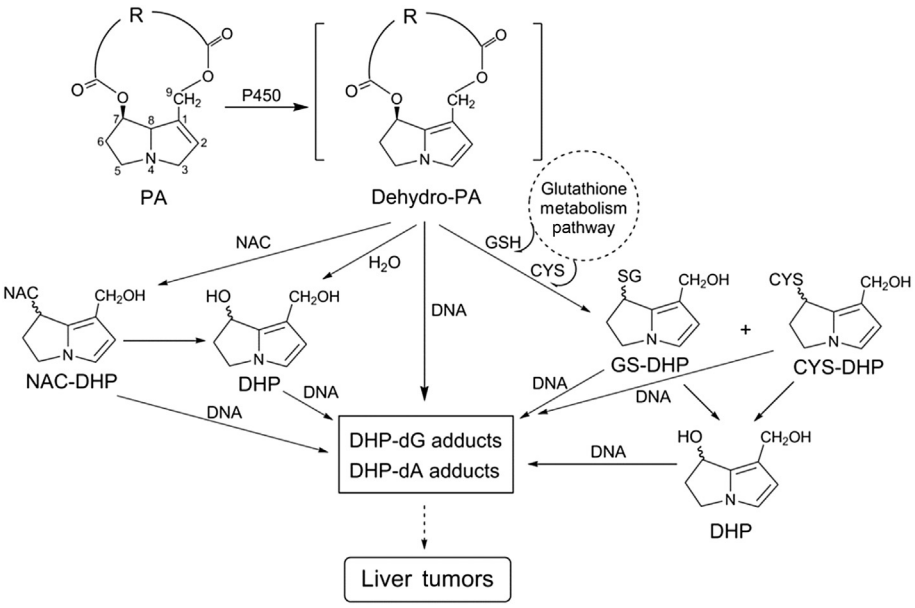

Figure 11 – The proposed general metabolic activation pathways leading to the formation of DNA adducts and the potential initiation of PA-induced liver tumors. dA = 2′-deoxyadenosine, dG = 2′-deoxyguanosine, DHP = (±)-6,7-dihydro-7-hydroxy-1-hydroxymethyl-5*H*-pyrrolizine, NAC = *N*-acetylcysteine, PA = pyrrolizidine alkaloids.

in a time-dependent manner. The representative LC/MS/MS SRM chromatograms of the DHP-dG and DHP-dA adducts formed from the reaction of 7-NAC-DHP with calf thymus DNA for 3 days are shown in Fig. 10. The results clearly indicate that all of these DHP-dG and DHP-dA adducts were formed.

4. Discussion

It has been established that the metabolism of PAs to the reactive dehydro-PA metabolites is catalyzed by cytochrome P-450 enzymes [6,15,29,30]. In order to exert the enzymatic functions, cytochrome P-450 enzymes require NADPH as a cofactor. In this study, we found that metabolism of riddelliine and monocrotaline by human and rat liver microsomes, in the presence of *N*-acetylcysteine, generated 7-NAC-DHP. However, its formation was inhibited when the metabolism was conducted without the addition of NADPH. These results clearly indicate that 7-NAC-DHP was formed through the reaction of the dehydro-PA metabolite with *N*-acetylcysteine. Although 7-NAC-DHP was found in the urine of rats administered monocrotaline or senecionine [28], our results show for the first time that it is formed in the liver through the reaction of dehydromonocrotaline or dehydrosenecionine with 7-*N*-acetylcysteine.

We also determined that 7-NAC-DHP is capable of binding to deoxynucleic acids and calf thymus DNA. Reaction of 7-NAC-DHP with dG formed DHP-dG-1, DHP-dG-2, DHP-dG-3, and DHP-dG-4 adducts. Similarly, reaction with dA generated DHP-dA-1, DHP-dA-2, DHP-dA-3, and DHP-dA-4 adducts. Furthermore, reaction of 7-NAC-DHP with calf thymus DNA produced all the above-described DHP-dG and DHP-dA adducts (Figs. 9 and 10). These results indicate that 7-NAC-DHP is a reactive liver microsomal metabolite capable of alkylating 2′-deoxynuclic acids, e.g., dG and dA, as well as DNA. This is the first report to indicate that 7-NAC-DHP is a reactive metabolite that can lead to DNA adduct formation.

We recently demonstrated that both 7-GS-DHP and 7-cysteine-DHP can bind to DNA to form the same set of DNA adducts [26,27]. To date, all the known metabolites that have been shown to be capable of binding to DNA to form this set of DNA adducts (DHP-dG-3, DHP-dG-4, DHP-dA-3, and DHP-dA-4 adducts) are dehydro-PAs, DHP, 7-GS-DHP, 7-cysteine-DHP, and 7-NAC-DHP. This set of DHP-dG-3, DHP-dG-4, DHP-dA-3, and DHP-dA-4 adducts has been proposed to be a biomarker of PA exposure and potentially, a biomarker of PA-induced liver tumorigenicity [8]. Thus, based on our findings, we propose that there exist multiple metabolic activation pathways of carcinogenic PAs leading to the formation of pyrrolic DNA adducts and causing PA-induced liver tumors initiation. These proposed multiple activation pathways are illustrated in Fig. 11.

N-Acetylcysteine, the *N*-acetyl derivative of the amino acid L-cysteine, is a natural thiol-containing antioxidant and a precursor for the synthesis of cysteine and glutathione in the body. N-acetylcysteine, cysteine, and glutathione possess a sulfhydryl (thiol) group that confers antioxidant effects to scavenge free radicals generated in the body. Since *N*-acetylcysteine, cysteine, and glutathione are commercial dietary supplements, uptake of these antioxidants may increase the formation of 7-*N*-acetylcysteine, 7-cysteine-DHP, and 7-glutathione-DHP in humans who are exposed to PAs and thus may cause adverse effects, which warrants further investigation.

We have studied the synthesis, stability, solubility, and reactivity of a series of secondary pyrrolic metabolites and derivatives, including 7-NAC-DHP, 7-cysteine-DHP [27], 7-glutathione-DHP [26], 7,9-diglutathione-DHP [31], and 7-

valine-DHP [32]. We have determined that among these secondary pyrrolic metabolites, 7-NAC-DHP is less water soluble and is relatively more stable. Thus, it is highly possible this metabolite can be relatively easily translocated out of the liver to other organs and exerts extrahepatic toxicity.

Conflicts of interest

The authors declare no conflict of interest.

Acknowledgments

We thank Dr. F. Beland for critical review of this manuscript. This research was supported in part by appointments (X.H.; L.M.) to the Postgraduate Research Program at the NCTR administered by the Oak Ridge Institute for Science and Education through an interagency agreement between the U.S. Department of Energy and the FDA. This article is not an official U.S. Food and Drug Administration (FDA) guidance or policy statement. No official support or endorsement by the U.S. FDA is intended or should be inferred. The authors declare no competing financial interest.

REFERENCES

[1] Edgar JA, Molyneux RJ, Colegate SM. Pyrrolizidine alkaloids: potential role in the etiology of cancers, pulmonary hypertension, congenital anomalies, and liver disease. Chem Res Toxicol 2015;28:4–20.
[2] Fu PP, Chou MW, Xia Q, Yang Y-C, Yan J, Doerge DR, Chan PC. Genotoxic pyrrolizidine alkaloids and pyrrolizidine alkaloid N-oxides—mechanisms leading to DNA adduct formation and tumorigenicity. J Environ Sci Health, Part C 2001;19:353–85.
[3] Fu PP, Xia Q, Lin G, Chou MW. Pyrrolizidine alkaloids–genotoxicity, metabolism enzymes, metabolic activation, and mechanisms. Drug Metab Rev 2004;36:1–55.
[4] Fu PP, Yang Y-C, Xia Q, Chou MW, Cui YY, Lin G. Pyrrolizidine alkaloids – tumorigenic components in Chinese herbal medicines and dietary supplements. J Food Drug Anal 2002;10:198–211.
[5] Huxtable RJ. Human health implications of pyrrolizidine alkaloids and herbs containing them. In: Cheeke PR, editor. Alkaloids I. Boca Raton, FL: CRC Press; 1989. p. 41–86.
[6] Mattocks AR. Chemistry and Toxicology of Pyrrolizidine Alkaloids. London, NY: Academic Press; 1986.
[7] Roeder E. Medicinal plants in China containing pyrrolizidine alkaloids. Pharmazie 2000;55:711–26.
[8] Xia Q, Zhao Y, Von Tungeln LS, Doerge DR, Lin G, Cai L, Fu PP. Pyrrolizidine alkaloid-derived DNA adducts as a common biological biomarker of pyrrolizidine alkaloid-induced tumorigenicity. Chem Res Toxicol 2013;26:1384–96.
[9] Chou MW, Fu PP. Formation of DHP-derived DNA adducts in vivo from dietary supplements and chinese herbal plant extracts containing carcinogenic pyrrolizidine alkaloids. Toxicol Ind Health 2006;22:321–7.
[10] Fu PP, Chou MW, Churchwell M, Wang Y, Zhao Y, Xia Q, Gamboa da Costa G, Marques MM, Beland FA, Doerge DR. High-performance liquid chromatography electrospray ionization tandem mass spectrometry for the detection and quantitation of pyrrolizidine alkaloid-derived DNA adducts *in vitro* and *in vivo*. Chem Res Toxicol 2010;23:637–52.
[11] Wang YP, Fu PP, Chou MW. Metabolic activation of the tumorigenic pyrrolizidine alkaloid, retrorsine, leading to DNA adduct formation in vivo. Int J Environ Res Public Health 2005;2:74–9.
[12] Wang YP, Yan J, Beger RD, Fu PP, Chou MW. Metabolic activation of the tumorigenic pyrrolizidine alkaloid, monocrotaline, leading to DNA adduct formation in vivo. Cancer Lett 2005;226:27–35.
[13] Wang YP, Yan J, Fu PP, Chou MW. Human liver microsomal reduction of pyrrolizidine alkaloid N-oxides to form the corresponding carcinogenic parent alkaloid. Toxicol Lett 2005;155:411–20.
[14] Xia Q, Chou MW, Edgar JA, Doerge DR, Fu PP. Formation of DHP-derived DNA adducts from metabolic activation of the prototype heliotridine-type pyrrolizidine alkaloid, lasiocarpine. Cancer Lett 2006;231:138–45.
[15] Xia Q, Chou MW, Kadlubar FF, Chan P-C, Fu PP. Human liver microsomal metabolism and DNA adduct formation of the tumorigenic pyrrolizidine alkaloid, riddelliine. Chem Res Toxicol 2003;16:66–73.
[16] Xia Q, Chou MW, Lin G, Fu PP. Metabolic formation of DHP-derived DNA adducts from a representative otonecine type pyrrolizidine alkaloid clivorine and the extract of *Ligularia hodgsonnii* hook. Chem Res Toxicol 2004;17:702–8.
[17] Xia Q, Yan J, Chou MW, Fu PP. Formation of DHP-derived DNA adducts from metabolic activation of the prototype heliotridine-type pyrrolizidine alkaloid, heliotrine. Toxicol Lett 2008;178:77–82.
[18] Yan J, Xia Q, Chou MW, Fu PP. Metabolic activation of retronecine and retronecine N-oxide - formation of DHP-derived DNA adducts. Toxicol Ind Health 2008;24:181–8.
[19] Zhao Y, Xia Q, Gamboa da Costa G, Yu H, Cai L, Fu PP. Full structure assignments of pyrrolizidine alkaloid DNA adducts and mechanism of tumor initiation. Chem Res Toxicol 2012;25:1985–96.
[20] Cooper RA, Huxtable RJ. A simple procedure for determining the aqueous half-lives of pyrrolic metabolites of pyrrolizidine alkaloids. Toxicon 1996;34:604–7.
[21] Buhler DR, Miranda CL, Kedzierski B, Reed RL. Mechanisms for pyrrolizidine alkaloid activation and detoxification. Adv Exp Med Biol 1991;283:597–603.
[22] Lame MW, Morin D, Jones AD, Segall HJ, Wilson DW. Isolation and identification of a pyrrolic glutathione conjugate metabolite of the pyrrolizidine alkaloid monocrotaline. Toxicol Lett 1990;51:321–9.
[23] Lin G, Cui YY, Hawes EM. Microsomal formation of a pyrrolic alcohol glutathione conjugate of clivorine. Firm evidence for the formation of a pyrrolic metabolite of an otonecine-type pyrrolizidine alkaloid. Drug Metab Dispos 1998;26:181–4.
[24] Mattocks AR, Croswell S, Jukes R, Huxtable RJ. Identity of a biliary metabolite formed from monocrotaline in isolated, perfused rat liver. Toxicon 1991;29:409–15.
[25] Reed RL, Miranda CL, Kedzierski B, Henderson MC, Buhler DR. Microsomal formation of a pyrrolic alcohol glutathione conjugate of the pyrrolizidine alkaloid senecionine. Xenobiotica 1992;22:1321–7.
[26] Xia Q, Ma L, He X, Cai L, Fu PP. 7-Glutathione pyrrole adduct: a potential DNA reactive metabolite of pyrrolizidine alkaloids. Chem Res Toxicol 2015;28:615–20.
[27] He X, Xia Q, Ma L, Fu PP. 7-Cysteinyl-Pyrrole Conjugate-a New Potential DNA Reactive Metabolite of Pyrrolizidine Alkaloids. J Environ Sci Health, Part C 2016;34:57–76.
[28] Estep JE, Lame MW, Jones AD, Segall HJ. N-acetylcysteine-conjugated pyrrole identified in rat urine following

administration of two pyrrolizidine alkaloids, monocrotaline and senecionine. Toxicol Lett 1990;54:61–9.
[29] Ruan J, Yang M, Fu P, Ye Y, Lin G. Metabolic activation of pyrrolizidine alkaloids: insights into the structural and enzymatic basis. Chem Res Toxicol 2014;27:1030–9.
[30] Li N, Xia Q, Ruan J, Fu PP, Lin G. Hepatotoxicity and tumorigenicity induced by metabolic activation of pyrrolizidine alkaloids in herbs. Current Drug Metab 2011;12:823–34.
[31] Ma L, Zhao H, Xia Q, Cai L, Fu PP. Synthesis and phototoxicity of isomeric 7, 9-diglutathione pyrrole adducts: Formation of reactive oxygen species and induction of lipid peroxidation. J Food Drug Anal 2015;23:577–86.
[32] Jiang X, Wang S, Zhao Y, Xia Q, Cai L, Sun X, Fu PP. Absolute configuration, stability, and interconversion of 6, 7-dihydro-7-hydroxy-1-hydroxymethyl-5H-pyrrolizine valine adducts and their phenylthiohydantoin derivatives. J Food Drug Anal 2015;23:318–26.